THE JOURNAL OF BIOLOGICAL CHEMISTRY
Vol. 277, No. 21, Issue of May 24, pp. 18777–18784, 2002

Printed in U.S.A.

GSTB1-1 from *Proteus mirabilis*

A SNAPSHOT OF AN ENZYME IN THE EVOLUTIONARY PATHWAY FROM A REDOX ENZYME TO A CONJUGATING ENZYME*

Received for publication, February 4, 2002, and in revised form, March 4, 2002
Published, JBC Papers in Press, March 11, 2002, DOI 10.1074/jbc.M201137200

Anna Maria Caccuri,[a] Giovanni Antonini,[b,c,d] Nerino Allocati,[e,f] Carmine Di Ilio,[e,f] Francesca De Maria,[a] Federica Innocenti,[a] Michael W. Parker,[g] Michele Masulli,[e] Mario Lo Bello,[a] Paola Turella,[a,h] Giorgio Federici,[i] and Giorgio Ricci[a,d,f,i,j]

From the From [a]Department of Biology, University of Rome, Tor Vergata, 00133 Rome, Italy, the [b]Department of Basic and Applied Biology, University of L'Aquila, 67010 L'Aquila, Italy, the [c]Department of Biology, University of Rome Three, 00145 Rome, Italy, the [e]Department of Biomedical Science, University of Chieti, G. D'Annunzio, 66013 Chieti, Italy, the [g]Biota Structural Biology Laboratory, St. Vincent's Institute of Medical Research, 9 Princes St., Fitzroy, Victoria 3065, Australia, the [h]Department of Biochemical Sciences, University of Rome, La Sapienza, 00185 Rome, Italy, and the [i]Children's Hospital Istituto di Ricerca e Cura a Carattere Scientifico, Bambin Gesu, 00165 Rome, Italy

The native form of the bacterial glutathione transferase B1-1 (EC 2.5.1.18) is characterized by one glutathione (GSH) molecule covalently linked to Cys-10. This peculiar disulfide, only found in the Beta and Omega class glutathione *S*-transferases (GSTs) but absent in all other GSTs, prompts questions about its role and how GSH can be activated and utilized in the reaction normally performed by GSTs. Stopped-flow and spectroscopic experiments suggest that, in the native enzyme (GSTB1-1ox), a second GSH molecule is present, albeit transiently, in the active site. This second GSH binds to the enzyme through a bimolecular interaction followed by a fast thiol-disulfide exchange with the covalently bound GSH. The apparent pK_a of the non-covalently bound GSH is lowered from 9.0 to 6.4 ± 0.2 in similar fashion to other GSTs. The reduced form of GSTB1-1 (GSTB1-1red) binds GSH 100-fold faster and also induces a more active deprotonation of the substrate with an apparent pK_a of 5.2 ± 0.1. Apparently, the absence of the mixed disulfide does not affect k_{cat} and K_m values in the GST conjugation activity, which is rate-limited by the chemical step both in GSTB1-1red and in GSTB1-1ox. However, GSTB1-1ox follows a steady-state random sequential mechanism whereas a rapid-equilibrium random sequential mechanism is adopted by GSTB1-1red. Remarkably, GSTB1-1ox and GSTB1-1red are equally able to catalyze a glutaredoxin-like catalysis using cysteine *S*-sulfate and hydroxyethyl disulfide as substrates. Cys-10 is an essential residue in this redox activity, and its replacement by alanine abolishes this enzymatic activity completely. It appears that GSTB1-1 behaves like an "intermediate enzyme" between the thiol-disulfide oxidoreductase and the GST superfamilies.

Cytosolic glutathione *S*-transferases (GSTs,[1] EC 2.5.1.18) are a superfamily of multifunctional enzymes involved in the cellular detoxification of many endobiotic and xenobiotic compounds (1, 2). They are dimeric proteins grouped into at least ten gene-independent classes named Alpha, Beta, Delta, Kappa, Pi, Mu, Theta, Zeta, Sigma, and Omega, on the basis of different amino acid sequences and substrate specificities (3–11). Several x-ray crystal structures, with representatives of nearly every class, have been solved in the last years, showing that all GSTs have similar tertiary structure and active site topography (11–20). A prominent catalytic activity performed by the eucaryotic GSTs (in particular by the Alpha, Mu, Pi, Theta, and Sigma GSTs) is the conjugation of glutathione (GSH) to a number of toxic electrophilic compounds, thus promoting their excretion (1, 2). This activity is due to the activation of the sulfhydryl group of GSH, which is stabilized in the reactive thiolate form by a tyrosine residue (Alpha, Pi, Mu, and Sigma classes) or by a serine residue (Delta, Theta, and Zeta classes) in the proximity of the GSH sulfur atom (10, 21–25). GSTs are, in fact, multifunctional enzymes devoted to various aspects of cell defense. A few selected GSTs are able to catalyze a GSH-dependent reduction of organic hydroperoxides (26) and to act as a binding protein of hydrophobic molecules like steroids and heme (27). Recent advances revealed that GST P_i is involved in the response of mammalian cells to different forms of stress and in particular to the regulation of Jun kinase protein (28, 29). In addition, Theta and Omega GST classes may play a role in the protection of mammalian cells from apoptosis (30, 31). The recently discovered procaryotic GSTs represent an atypical GST class. A prototype of this class is GSTB1-1 from *Proteus mirabilis*, which displays poor conjugation activity, lacks substrate specificity (32), does not use Tyr or Ser residues in the activation of the substrate (33), and is localized in the periplasmic space (34). A singular feature of this bacterial enzyme is the presence of a mixed disulfide between one GSH molecule and the sulfhydryl group of Cys-10, which resides in the GSH binding site (G-site). The GSH mol-

* The costs of publication of this article were defrayed in part by the payment of page charges. This article must therefore be hereby marked "*advertisement*" in accordance with 18 U.S.C. Section 1734 solely to indicate this fact.

[d] Supported by the National Research Council of Italy (Target Project on Biotechnology).

[f] Supported by the Ministry of the University and Scientific and Technological Research PRIN2000.

[j] To whom correspondence should be addressed: Dept. of Biology, University of Rome, Tor Vergata, Viale della Ricerca Scientifica, Rome RM 00133, Italy. Tel.: 39-06-72594379; Fax: 39-06-72594328; E-mail: riccig@uniroma2.it.

[1] The abbreviations used are: GST, glutathione transferase; GSTB1-1ox, oxidized bacterial glutathione transferase; GSTB1-1red, reduced bacterial glutathione transferase; GSH, glutathione; GSSG glutathione disulfide; CDNB, 1-chloro-2,4-dinitrobenzene; FDNB, 1-fluoro-2,4-dinitrobenzene; NBD-Cl, 7-chloro-4-nitrobenzo-2-oxa-1,3-diazole; NBD-F, 7-fluoro-4-nitrobenzo-2-oxa-1,3-diazole; $CysSO_3^-$, cysteine *S*-sulfate; HEDS, hydroxyethyl disulfide; G-site, GSH binding site; Cys-10-SG, Cys-10-glutathione mixed disulfide.

ecule is located in the G-site in a fashion similar to that observed in the active site of all other GSTs where it is anchored to the protein by means of eleven polar interactions and of several hydrophobic links (19). The presence of a covalently bound GSH in the G-site is a paradoxical finding in view of the observed conjugation activity of this enzyme. In fact, the sulfur atom of GSH, in this oxidized state, cannot interact with the electrophilic center of the co-substrate, and there was no evidence of a second GSH molecule in the G-site from the crystal structure. In a preceding report (35), we demonstrated that the Cys-10-SG mixed disulfide is characterized by a high reactivity. It exchanges rapidly with external GSH pools in a futile redox cycle, which only replaces the bound GSH with the free GSH so that the enzyme is mainly recovered as an oxidized enzyme. When GSH is removed from the disulfide, Cys-10 displays a relatively high pK_a value of 8.0, and it is rapidly converted into the oxidized form by trace amounts of GSSG even in the presence of an excess of GSH. The redox properties of Cys-10 are reminiscent of the scenario found in the thiol-disulfide oxidoreductase superfamily, from which all GSTs have probably evolved in the past (36). The $\beta\alpha\beta\alpha\beta\beta\alpha$ motif of the N-terminal domain of thioredoxins and glutaredoxins superimposes well with the N-terminal domain of GSTs, and the active site of the thiol-disulfide oxidoreductase is also characterized by one or two essential cysteine residues that easily form a stable or transient mixed disulfide during catalysis (37, 38). In this context, the recently discovered human GST Omega class (11), which almost lacks any sign of conjugation activity, but is able to catalyze redox reactions with disulfides, seems to confirm an evolutionary link between the two superfamilies. Remarkably, this enzyme also displays a peculiar mixed disulfide between Cys-32 and GSH. The present report demonstrates that GSTB1-1 is able to perform both a conjugation activity and redox activity with comparable efficiency, and in the latter activity Cys-10 is shown to be an essential residue. Stopped-flow data and steady-state kinetic experiments, carried out to clarify the mechanisms of the substrate activation and catalysis, reveal unexpected findings that support the suggestion that GSTB1-1 represents a transition enzyme between the thiol-disulfide oxidoreductase superfamily and the GST superfamily.

EXPERIMENTAL PROCEDURES

Materials—Glutathione (GSH), oxidized glutathione (GSSG), 1-chloro-2,4-dinitrobenzene (CDNB), 1-fluoro-2,4-dinitrobenzene (FDNB), and cysteine *S*-sulfate ($CysSO_3^-$) were obtained from Sigma Chemical Co.; hydroxyethyl disulfide (HEDS) was obtained from Aldrich; and 7-chloro-4-nitrobenzo-2-oxa-1,3-diazole (NBD-Cl) and 7-fluoro-4-nitrobenzo-2-oxa-1,3-diazole (NBD-F) were obtained from Fluka.

Enzymes—The recombinant GSTB1-1 and C10A mutant enzymes were expressed in *Escherichia coli* and purified as previously described (32, 33). The purified GSTB1-1 is always recovered as a mixed disulfide between the sulfur atom of Cys-10 residue and the GSH thiol (GSTB1-1ox). Reduction of the disulfide was obtained after 30-min incubation with 50 mM dithiothreitol at 37 °C and pH 7.0. GSTB1-1red was separated from the excess of reducing reagents by a Sephadex G-25 column and equilibrated with 0.01 M potassium phosphate buffer, pH 7.0. Protein concentration was calculated from the absorbance at 280 nm assuming an $\epsilon_{1\ mg/ml}$ of 1.02. The extinction coefficient was calculated on the basis of the amino acid sequence as reported by Gill *et al.* (39) and confirmed by the bicinchoninic acid method (Pierce). A molecular mass of 22.5 kDa per GST subunit was used in the calculations (4).

GSH Binding to GSTB1-1ox and GSTB1-1red—Binding of GSH to GSTB1-1ox and GSTB1-1red in 0.1 M potassium phosphate buffer, pH 7.0, was measured in a single photon counting spectrofluorometer (Fluoromax, S.A. Instrument, Paris, France) with a sample holder set at 25 °C. Excitation was at 295 nm and emission was at 350 nm. In a typical experiment, fluorescence intensity was measured before and after the addition of suitable amounts of GSH (from 0.05 to 3 mM) to 4.4 μM enzyme. Experimental data were corrected both for dilution and for inner filter effects and fitted to Equation 1,

$$F_L = F_o + (F_{max} - F_o)/(1 + ([S]_{0.5}/[S]^{n_H})) \quad \text{(Eq. 1)}$$

where F_o is the protein fluorescence in the absence of GSH, F_L is the protein fluorescence in the presence of a given amount of GSH; F_{max} is the protein fluorescence at saturating GSH concentrations, and n_H is the Hill coefficient.

Spectroscopic Evidence for a Forced Deprotonation of the Bound GSH—Difference spectra of GSH thiolate bound to GSTB1-1ox, GSTB1-1red, and C10A mutant enzymes were obtained with a Kontron double-beam Uvikon 940 spectrophotometer thermostatted at 25 °C. In a typical experiment 1 mM GSH was added to the enzyme (15 μM) in 0.1 M potassium phosphate buffer, pH 7.0. Spectra were corrected for the contribution of free GSH and free enzyme. The amount of thiolate was calculated by assuming an $\epsilon_{240\ nm}$ of 5000 $M^{-1}\ cm^{-1}$. Experiments at different pH values were carried out using the following buffers (0.1 M): sodium acetate buffer (pH 5.0 and 5.5) and potassium phosphate buffer (between pH 6.0 and 8.0). pK_a values for GSTB1-1ox and GSTB1-1red were calculated by fitting the spectral data to Equation 2,

$$A_{240\ nm} = (A^{lim}_{240\ nm} \times 10^{-pKa} + A^{min}_{240\ nm} \times 10^{-pH})/(10^{-pKa} + 10^{-pH}) \quad \text{(Eq. 2)}$$

where $A^{lim}_{240\ nm}$ is the limiting thiolate absorbance at alkaline pH values and $A^{min}_{240\ nm}$ is the residual thiolate absorbance at acidic pH values.

Kinetics of the Binding of GSH to GSTB1-1—Rapid kinetic experiments were performed on an Applied Photophysics Kinetic spectrometer stopped-flow instrument equipped with a thermostatted 1-cm light path observation chamber. Binding of GSH to GSTB1-1ox, GSTB1-1red, and C10A mutant enzymes was studied at 5 °C and 25 °C by rapid mixing of the enzyme (50–100 μM in 0.01 M potassium phosphate buffer, pH 7.0) with the same volume of GSH (from 2 to 20 mM) in (50:50:50 mM) phosphate-acetate-borate buffer, pH 7.0. Binding of GSH was monitored by following the increase of the intrinsic fluorescence of the protein and the increase of the absorbance at 240 nm due to the ionization of the bound GSH. Experimental traces were fitted to a single-exponential equation, and pseudo first-order kinetic constants were calculated at different GSH concentrations.

Conjugation Activity—Standard GST activity, with CDNB (1 mM) or NBD-Cl (0.1 mM) as co-substrates, was measured at 25 °C in (50:50:50) mM phosphate-acetate-borate buffer, pH 6.5, containing 5 mM GSH. The activity was assayed spectrophotometrically by following the enzymatic product at 340 nm (ϵ = 9600 $M^{-1}\ cm^{-1}$) for CDNB and at 419 nm (ϵ = 14,500 $M^{-1}\ cm^{-1}$) for NBD-Cl. Steady-state kinetic experiments with GSTB1-1ox and CDNB as co-substrate, were performed at pH 7.0 and 25 °C by varying CDNB from 0.4 to 2 mM and GSH from 0.1 to 5 mM over a matrix of 50 substrate concentrations. Steady-state kinetic experiments, with GSTB1-1red and CDNB as co-substrate, were performed at pH 7.0 and 25 °C by varying CDNB from 0.1 to 1 mM and GSH from 0.2 to 5 mM over a matrix of 50 substrate concentrations.

The pH dependence of k_{cat} with GSTB1-1ox and GSTB1-1red was determined at 25 °C in (50:50:50) mM phosphate-acetate-borate buffers in the pH range 4.5–8.0. With NBD-Cl as co-substrate, GSH and NBD-Cl were kept constant at saturating concentrations (5 and 0.1 mM, respectively). With CDNB as co-substrate, the k_{cat} values were calculated by varying CDNB between 0.1 and 2 mM at fixed and saturating GSH concentrations (5 mM from pH 5.0 to 8.0 and 10 mM at pH 4.5). Data of k_{cat} *versus* pH were fitted to Equation 3,

$$k_{cat} = (k^{lim}_{cat} \times 10^{-pKa} + k^{min}_{cat} \times 10^{-pH})/(10^{-pKa} + 10^{-pH}) \quad \text{(Eq. 3)}$$

where k^{lim}_{cat} is the limiting value at alkaline pH values and k^{min}_{cat} is the residual k_{cat} observed at low pH values.

Fluoride/Chloride Leaving Group Substitution—Kinetic data were obtained at 25 °C and at fixed NBD-Cl or NBD-F (0.05 mM) and GSH (2 mM) concentrations in 1 ml (final volume) of (50:50:50) phosphate-acetate-borate buffer, pH 5.0, containing suitable amounts of GSTB1-1ox or GSTB1-1red. The spontaneous reactions were evaluated under the same experimental conditions in the absence of the enzyme. Similar experiments were performed at fixed CDNB or FDNB (1 mM) and GSH (1 mM) concentrations in 1 ml (final volume) of (50:50:50) phosphate-acetate-borate buffer, pH 6.5, in the presence of suitable amounts of GSTB1-1red or GSTB1-1ox.

Thiol-disulfide Oxidoreductase Activity—The thiol-disulfide oxidoreductase activity was determined spectrophotometrically at 340 nm (30 °C), using the glutathione reductase/NADPH-coupled assay, according to Axelsson *et al.* (40). The assay mixture (1-ml final volume) contained: 0.14 M sodium phosphate, pH 7.6, 1 mM EDTA, 0.1 mM NADPH, 0.5 mM GSH, 2 units of glutathione reductase, 3 mM $CysSO_3^-$, and catalytic amounts of GSTB1-1. Thiol-disulfide oxidoreductase activity was also determined at 30 °C by using HEDS as co-substrate. The assay was performed in 1 ml of (50:50:50) mM phosphate-acetate-borate

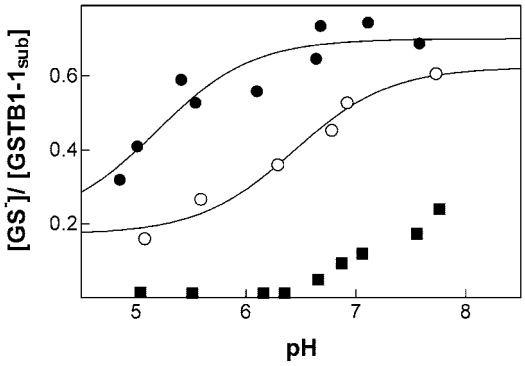

FIG. 1. **GSH thiolate formation in GSTB1-1ox and GSTB1-1red.** Difference spectra of GSH thiolate bound to GSTB1-1ox (○), GSTB1-1red (●), and C10A mutant enzyme (■) were obtained at different pH values and at 25 °C, as described under "Experimental Procedures," with 15 μM GST (active sites) and 1 mM GSH. The amount of thiolate formed at the G-site was calculated by assuming an $\epsilon_{240\ nm}$ of 5000 M^{-1} cm^{-1}. The *solid lines* are the best fit of data to Equation 2.

buffer, pH 7.0, containing 1 mM EDTA, 0.2 mM NADPH, 5 mM GSH, 4 units of glutathione reductase, 5 mM HEDS, and catalytic amounts of GSTB1-1. One unit of thiol-disulfide oxidoreductase activity is defined as the amount of enzyme that oxidizes 1 μmol of NADPH per min at 30 °C. The k_{cat} value was calculated at pH 7.0 at saturating GSH and HEDS concentrations. The amount of the glutathione reductase (used as the coupling enzyme) was always enough to avoid underestimation of the thiol-disulfide oxidoreductase reaction.

Steady-state kinetic analysis was performed with GSTB1-1ox and GSTB1-1red at pH 7.0 and 30 °C by varying both HEDS and GSH from 0.4 mM to 5 mM over a matrix of 40 substrate concentrations.

The dependence of the thiol-disulfide oxidoreductase activity on pH was determined at 30 °C in (50:50:50) mM phosphate-acetate buffers, between pH 4.5 and 7.5, in the conditions described above with both GSH and HEDS kept constant at 5 mM concentration. Experimental data were fitted to Equation 4.

$$\Delta A/\min = \Delta A/\min^{lim}/(1 + 10^{(pKa - pH)}) \quad \text{(Eq. 4)}$$

RESULTS

Binding of GSH to GSTB1-1ox and GSTB1-1red—Isothermic binding of GSH to GSTB1-1 has been studied at 25 °C and pH 7.0 by using the perturbation of the intrinsic fluorescence of the protein at different GSH concentrations. The fluorescence perturbation observed for GSTB1-1ox after GSH addition is a first indication that the substrate binds to the enzyme even when the mixed disulfide Cys-10-SG is present in the active site. The possibility of a quantitative reduction of this disulfide by GSH in the binding experiments can be ruled out on the basis of preceding studies indicating that more than 90% of GSTB1-1ox is recovered in the presence of 500 mM GSH (35). Fluorescence data, fitted to Equation 1, give K_D^{GSH} values of 1.3 ± 0.2 mM and 1.0 ± 0.2 mM for GSTB1-1ox and GSTB1-1red, respectively. The Hill coefficients of 1 and 0.9 for the two forms are indicative of a nearly non-cooperative binding mechanism.

GSH Activation in GSTB1-1ox, GSTB1-1red, and C10A Mutant—Fig. 1 shows the pH dependence of the thiolate absorption band at 240 nm obtained by the differential UV spectrum of GSTB1-1ox and GSTB1-1red in the presence of non-saturating GSH (1 mM). Higher GSH concentrations cannot be used because of the large spectral contribution due to the spontaneous ionization of GSH at alkaline pH values. The apparent pK_a value for the bound GSH is 6.4 ± 0.2 for GSTB1-1ox and 5.2 ± 0.1 for GSTB1-1red (Table I), close to the pK_a values found for Alpha, Pi, Mu, and Theta class GSTs (23–25). The occurrence of two different pK_a values is a further indication that a second molecule of GSH binds to the G-site of GSTB1-1ox and that this oxidized enzyme is not reduced by the external GSH.

TABLE I
pK_a values of sulfhydryl group of GSH bound to GSTB1–1 obtained by differential UV spectroscopy at equilibrium

	GSTB1–1ox	GSTB1–1red	C10A
pK_a	6.4 ± 0.2	5.2 ± 0.1	≥7.3

TABLE II
Kinetics of GSH binding

Temperature	k_{on}	k_{off}	K_D
	M^{-1} s^{-1}	s^{-1}	mM
GSTB1–1ox			
5 °C	(0.53 ± 0.05) × 10^3	0.83 ± 0.33	1.6 ± 0.4
25 °C	(1.22 ± 0.07) × 10^3	2.24 ± 0.40	1.8 ± 0.5
25 °C			1.3 ± 0.2[a]
GSTB1–1red			
5 °C	(192 ± 9) × 10^3	150 ± 27	0.8 ± 0.2
25 °C			1.0 ± 0.2[a]

[a] Data were obtained by fluorescence experiments at equilibrium.

By assuming an $\epsilon_{240\ nm}$ of 5000 M^{-1} cm^{-1} for the ionized GSH, the limiting value at alkaline pH values and at 1 mM GSH is 0.6 and 0.7 GS^- equivalents per active site for GSTB1-1ox and GSTB1-1red, respectively. At saturating GSH concentration and on the basis of the apparent K_D values, about one GSH thiolate per subunit can be calculated. A peculiar finding, never observed in other GSTs classes such as Alpha, Pi, Mu, and Theta, is the persistence of a residual amount of ionized GSH even at low pH values (about 0.3 equivalent per active site). In the C10A mutant (Fig. 1), substitution of cysteine with alanine shifts the apparent pK_a of GSH to a value ≥ 7.3 and eliminates the residual GSH ionization at low pH values suggesting a role of the Cys-10 residue in the thiolate stabilization.

GSH Binding Mechanism—Rapid kinetic experiments were performed to dissect the binding mechanism of GSH to GSTB1-1ox, GSTB1-1red, and C10A mutant enzymes. The perturbation of the intrinsic fluorescence at 340 nm due to the substrate interaction and the absorbance increase at 240 nm due to the thiolate formation have been utilized in these kinetic experiments. In the case of GSTB1-1red, k_{obs} values, calculated at 5 °C and pH 7.0, follow a linear dependence on GSH concentration up to 5 mM, and the fluorescence perturbation is synchronous with the thiolate formation (Fig. 2). Linear regression analysis gives k_{on} = (192 ± 9) × 10^3 $M^{-1}s^{-1}$ and k_{off} = 150 ± 27 s^{-1}. The resulting K_D is 0.8 ± 0.2 mM, close to the value found by fluorometric experiments at equilibrium (see Table II). Thus, the binding mechanism can be modeled as a simple bimolecular interaction between the enzyme and GSH to give the final activated complex (Scheme 1). Rates of GSH binding and release are temperature-dependent, and at 25 °C k_{obs} values are almost triplicated, although the very fast kinetics allowed rough estimate of data.

In the case of GSTB1-1ox, the presence of a GSH molecule covalently linked in the active site makes a different and more complex scenario. At pH 7.0 and 5 °C, the fluorescence perturbation is synchronous with the thiolate formation, and k_{obs} values are also linearly dependent on GSH concentration (Fig. 2). However, the microscopic kinetic constants are about two orders of magnitude lower than those found for the reduced enzyme. Linear regression analysis gives k_{on} = (0.53 ± 0.05) × 10^3 $M^{-1}s^{-1}$ and k_{off} = 0.83 ± 0.33 s^{-1}. The dissociation constant (K_D) is 1.6 ± 0.4 mM, close to the value obtained by fluorescence binding data at equilibrium (Table II). It is likely that the presence of the mixed disulfide Cys-10-SG causes a more difficult access and release of the second GSH molecule into and out of the G-site. Kinetics of the GSH binding process is also temperature-dependent, *i.e.* at 25 °C k_{on} is (1.22 ± 0.07) × 10^3

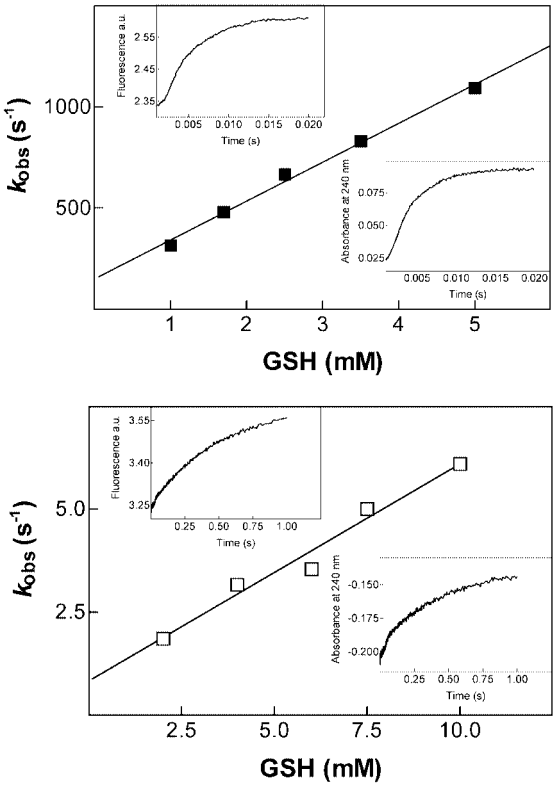

FIG. 2. **Kinetics of GSH binding to GSTB1-1ox and GSTB1-1red.** Binding experiments were performed, at pH 7.0 and 5 °C, by rapid mixing GSTB1-1 (100 μM) with the same volume of GSH (from 2 to 20 mM). The observed rate constants (k_{obs}) for the GSH binding were calculated by following the increase of the intrinsic fluorescence of the protein due to the substrate interaction and from the increase of the absorbance at 240 nm due to the ionization of bound GSH. With GSTB1-1red, the rates for the GSH binding and ionization were too fast to be accurately measured above 5 mM GSH (final concentration). The fluorescence perturbation is synchronous with the thiolate formation; therefore, only fluorescence data have been reported. Data shown in the figure represent the mean of three different experiments; the standard error for each point does not exceed 5%. The *solid lines* are the best fit of the experimental data to the GSH binding mechanism shown in Scheme 1 for GSTB1-1red (■) and in Scheme 2 for GSTB1-1ox (□). *Insets* show the experimental traces obtained at 340 nm and at 240 nm by rapid mixing either GSTB1-1ox or GSTB1-1red with the same volume of GSH (2 mM).

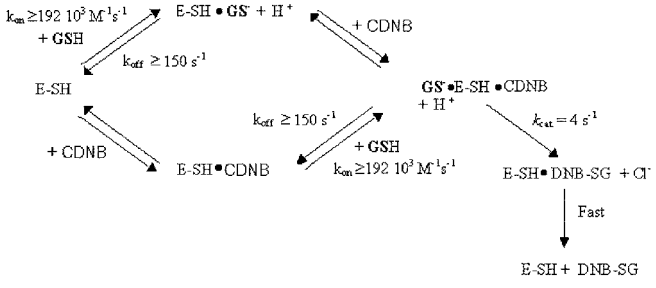

SCHEME 1. **Catalytic mechanism for GSTB1-1red in the conjugation reaction (25 °C).**

$M^{-1}s^{-1}$ and k_{off} is 2.24 ± 0.40 s^{-1}, with a dissociation constant (K_D) of 1.8 ± 0.5 mM (Table II). A reasonable binding mechanism is proposed (Scheme 2) on the basis of the present kinetic data and also of preceding findings (35) showing a rapid exchange between the free GSH and the GSH covalently bound in the active site ($k_2 = k_{-2} \geq 13\ s^{-1}$). In the proposed mechanism, the k_2 value has been drawn from displacement kinetics of the Cys-10-thiopiridine mixed disulfide by GSH (35). In addition, the possibility that the GSTB1-1ox·GS^- complex is the favorite species in a fast equilibrium with the reduced enzyme is also

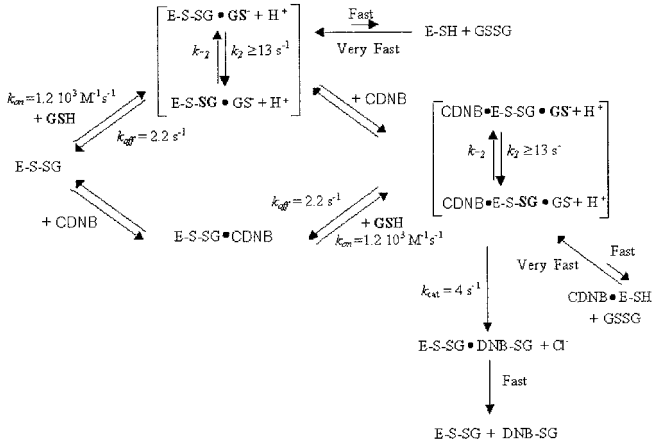

SCHEME 2. **Catalytic mechanism for GSTB1-1ox in the conjugation reaction (25 °C).**

reported in Scheme 2, based on previous observations (35). Replacement of the Cys-10 residue with alanine has little influence on the GSH binding kinetics; the k_{obs} value for the C10A mutant enzyme, at 25 °C, pH 7.0, and 1 mM GSH (k_{obs} = 461 s^{-1}), is close to that observed with GSTB1-1red (k_{obs} = 1000 s^{-1}) and about two order of magnitude higher than that obtained with GSTB1-1ox (k_{obs} = 5.3 s^{-1}) under the same experimental conditions.

Steady-state Kinetics of the Conjugation Reaction—GSTB1-1ox and GSTB1-1red show very similar specific activities with CDNB as co-substrate and close apparent K_m values (Table III). Similar specific activities have been also found using NBD-Cl as co-substrate. Notably, the apparent K_m^{GSH} value, with NBD-Cl as co-substrate, is about 0.7 mM and the apparent $K_m^{NBD\text{-}Cl}$ value is ≤5 μM for both GSTB1-1red and GSTB1-1ox (Table III). Kinetic data, obtained at pH 7.0 with GSTB1-1ox by varying both CDNB and GSH over a matrix of 50 substrate concentrations (see "Experimental Procedures"), are compatible with a sequential mechanism by which all substrates bind to the enzyme before the first product is formed. Deviation from linearity, observed at GSH concentrations higher than 1 mM (variable substrate) and CDNB concentrations lower than 1 mM (fixed substrate), may be diagnostic for cooperativity. On the other hand, GSH binding to GSTB1-1ox shows a non-cooperative interaction; thus, deviation from linearity observed with GSTB1-1ox could be due to a steady-state random sequential mechanism in which the formation of the *E*·GSH binary complex is the preferred pathway (41). GSTB1-1red shows a different kinetic scenario, because no apparent deviation from linearity is observed at high GSH concentrations; this kinetics is compatible to a rapid equilibrium sequential mechanism. Unexpectedly, we observed that GSSG was a strong inhibitor of the CDNB-GSH catalyzed reaction. GSSG behaves as a competitive inhibitor toward GSH with a K_i value of about 30 μM at pH 6.5.

Activity of C10A Mutant—The effect of replacement of the Cys-10 residue with alanine depends on the nature of the co-substrate. In fact, the specific activity found in C10A mutant enzyme with CDNB (1 mM) and GSH (5 mM) at pH 6.5 is 1.8 units/mg, a value comparable to that observed for the native enzyme (2.3 units/mg). Conversely, NBD-Cl becomes a poor co-substrate for the C10A mutant enzyme, which shows a specific activity of 0.05 unit/mg at pH 6.5 with 0.1 mM NBD-Cl and 5 mM GSH. These data confirm that the role of the Cys-10 residue is important but not essential for the conjugation activity, as also previously indicated (33).

pH Dependence of k_{cat}—The pH dependence of k_{cat} values in the reaction catalyzed by GSTB1-1ox and GSTB1-1red using NBD-Cl as co-substrate is shown in Fig. 3. An apparent pK_a

TABLE III
Steady-state kinetic parameters using CDNB and NBD-Cl as co-substrates

	GSTB1–1ox	GSTB1–1red
GSH-CDNB reaction		
S.A.[a]	2.3 units/mg	2.0 units/mg
K_m^{CDNB}	(2.5 ± 0.5) mM	(2.0 ± 0.5) mM
K_m^{GSH}	(0.34 ± 0.04) mM[b]	(0.30 ± 0.06) mM
GSH-NBD-Cl reaction		
S.A.[a]	2.6 units/mg	2.4 units/mg
$K_m^{NBD\text{-}Cl}$	≤5 μM	≤5 μM
K_m^{GSH}	(0.7 ± 0.2) mM	(0.8 ± 0.2) mM

[a] The specific activity (S.A.) for conjugation reaction, was measured at 25 °C in (50:50:50 mM) phosphate-acetate-borate buffer, pH 6.5, containing 5 mM GSH and CDNB (1 mM) or NBD-Cl (0.1 mM) as co-substrates.

[b] Due to the non-Michaelian kinetic behavior, this value represents $[S]_{0.5}$ obtained by the Hill equation, $v = V_{max}/(1 + (K/[S]^{nH}))$ where $K^{1/nH})) = [S]_{0.5}$.

value of 5.8 ± 0.1 and a k_{cat}^{lim} value of 1.07 ± 0.03 s^{-1} were found for both enzymes. A similar apparent pK_a value of 6.3 ± 0.3 was also observed in the case of GSTB1-1ox using CDNB as co-substrate whereas the k_{cat}^{lim} value of 3.7 ± 0.2 is about three times higher than that with NBD-Cl. Notably, with both CDNB and NBD-Cl, k_{cat} does not extrapolate to zero at acidic pH values. This behavior and the calculated pK_a values are reminiscent of the behavior observed for the forced deprotonation of GSH in the active site (see Fig. 1). This similarity suggests that the rate-limiting step of the catalyzed reaction with both CDNB and NBD-Cl likely depends on the deprotonation of GSH and that it could be the nucleophilic attack of the thiolate to the electrophilic center of the co-substrate.

Effect of the Leaving Group Substitution—A diagnostic test in evaluating the rate-limiting step in nucleophilic aromatic substitution reactions is the effect of different leaving groups on the kinetic parameters. By increasing the electronegativity of the leaving group, an increased k_{cat} value is a signal that the σ-complex formation is rate-limiting. The opposite effect is expected when the decomposition of the σ-complex is kinetically important. The effect of substitution of chlorine by the more electronegative fluorine was analyzed both in the NBD-Cl and in the CDNB molecules. The spontaneous reaction between NBD-F and GSH at pH 5.0 is about 13-fold faster than the same reaction with NBD-Cl, suggesting that the σ-complex formation is rate-limiting (42). Likewise, the $k_{cat}^{(NBD\text{-}F)}/k_{cat}^{(NBD\text{-}Cl)}$ ratio is 13 for the reaction catalyzed by both GSTB1-1ox and GSTB1-1red. Thus, the σ-complex formation is likely the rate-limiting step of the overall enzymatic reaction.

In the case of CDNB, the spontaneous reaction of GSH with FDNB at pH 6.5 is about 38-fold more rapid than with CDNB. In the catalyzed reaction the ratio k_{cat}^{F}/k_{cat}^{Cl} is about 9.0 with both GSTB1-1ox and GSTB1-1red, indicating that the rate-limiting step of the reaction is still the chemical event, but possibly a physical event has a comparable energy barrier.

Catalytic Mechanism of GSTB1-1 in the Conjugation Reaction—A possible catalytic mechanism for GSTB1-1red is reported (see Scheme 1), assuming that the binding of CDNB is fast and does not affect the binding of GSH. It collects the proposed GSH binding mechanism with the above kinetic findings: (*a*) the rate-limiting step is the chemical event, *i.e.* the nucleophilic attack of GSH thiolate to the co-substrate; (*b*) kinetics follows a rapid-equilibrium random sequential mechanism as supported by steady-state kinetic analysis and by the evidence that k_{cat} (4 s^{-1}; calculated at pH 7.0, 25 °C and at saturating GSH and CDNB concentrations) is much lower than k_{off} (≥150 s^{-1}, see Table II).

A possible catalytic mechanism for GSTB1-1ox is also reported below (Scheme 2), assuming that the binding of CDNB does not affect the binding of GSH. It collects the proposed GSH binding mechanism with the above kinetic findings: (*a*) the rate-limiting step is the chemical event; (*b*) kinetics follows a Briggs-Haldane steady-state random sequential mechanism as supported by steady-state kinetic analysis and by the evidence that k_{cat} (4 s^{-1}) is comparable to k_{off} (2.2 s^{-1}).

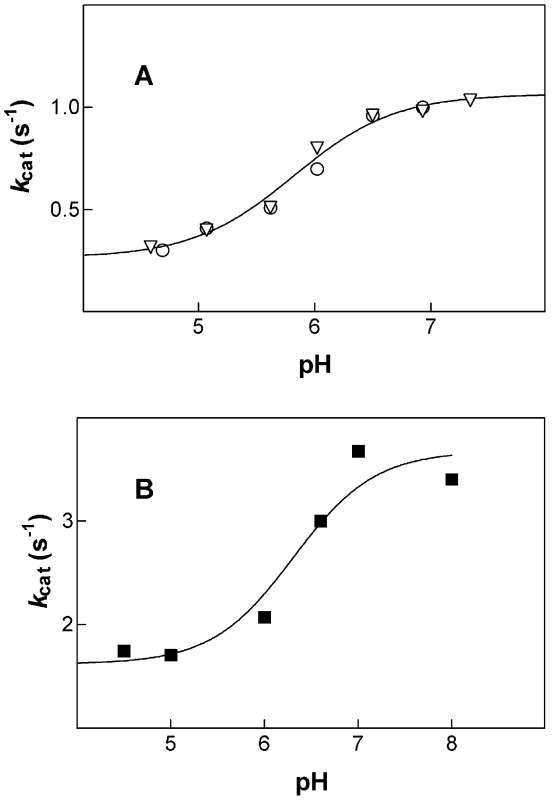

FIG. 3. **pH dependence of k_{cat} for the GSTB1-1-catalyzed conjugation of GSH with NBD-Cl and CDNB.** *A*, pH dependence of k_{cat} (s^{-1}) with GSTB1-1ox (▽), GSTB1-1red (○), and NBD-Cl as co-substrate. Kinetics parameters were obtained at 25 °C under saturating GSH and NBD-Cl concentrations (5 and 0.1 mM, respectively). *B*, pH dependence of k_{cat} (s^{-1}) with GSTB1-1ox (■) and CDNB as co-substrate. k_{cat} was obtained at 25 °C by varying CDNB between 0.1 and 2 mM at fixed and saturating GSH concentrations (5 mM from pH 5.0 to 8.0 and 10 mM at pH 4.5). Data shown in the figure represent the mean of three different experiments; the standard error for each point does not exceed 6%. Lines are the best fit of the experimental data to Equation 3.

Thiol-disulfide Oxidoreductase Activity—The GSH molecule covalently bound to the sulfur atom of Cys-10 and the structural similarities with the thiol-disulfide oxidoreductase superfamily, have suggested that the *in vivo* role of this bacterial GST could be as redox protein rather than conjugating enzyme (19), but this activity has never been demonstrated. Thus, the thiol-disulfide oxidoreductase activity was assayed with both $CysSO_3^-$ and HEDS, which are typical substrates for glutaredoxins, and the reaction was monitored by using the glutathione reductase/NADPH-coupled assay (Reaction 1),

$$CysSSO_3^- + 2GSH \longrightarrow CysSH + SO_3^{2-} + GSSG$$

$$EtSSEt + 2GSH \longrightarrow 2\ EtSH + GSSG$$

$$GSSG + NADPH + H^+ \xrightarrow{\text{Glutathione reductase}} 2\ GSH + NADP^+$$

REACTION 1

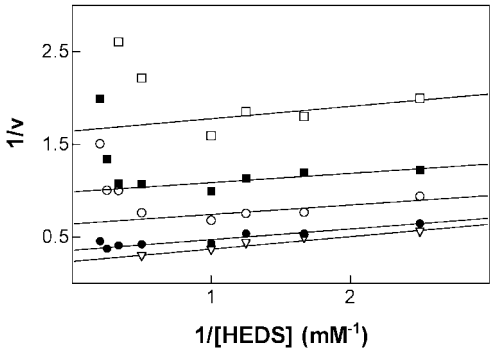

FIG. 4. **Reciprocal plots of the initial rate data for the thiol-disulfide oxidoreductase reaction with GSTB1-1ox.** Assay conditions are reported under "Experimental Procedures." HEDS was the varied substrate and GSH concentrations (millimolar) were fixed at 0.4, 0.6, 0.8, 2.0, and 5.0. Velocities were expressed as micromoles of NADPH·min^{-1}·mg^{-1}. Each data point represents the mean of three different experiments, and standard error does not exceed 8%.

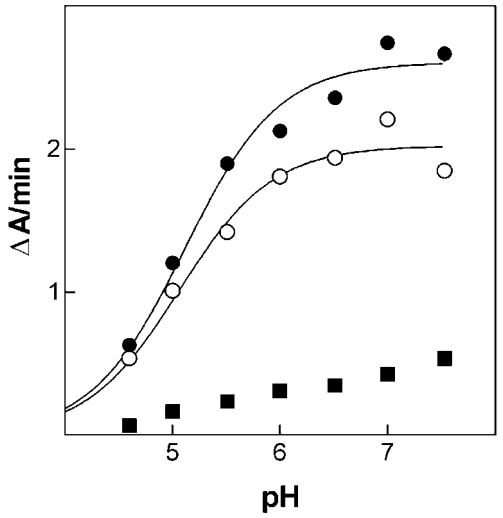

FIG. 5. **pH dependence of the thiol-disulfide oxidoreductase reaction.** The spontaneous (■) and the GSTB1-1red (●)- and GSTB1-1ox (○)-catalyzed reaction velocities were measured at 30 °C with both GSH and HEDS kept constant at 5 mM concentration. Lines are the best fit of the experimental data to Equation 4.

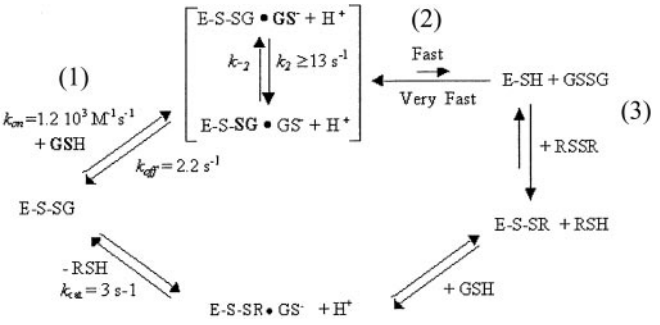

SCHEME 3. **Proposed kinetic mechanism for the thiol-disulfide oxidoreductase reaction of GSTB1-1.**

Both GSTB1-1ox and GSTB1-1red catalyze a glutathione-dependent thiol-disulfide oxidoreductase activity toward $CysSO_3^-$ with a specific activity of about 1 unit/mg under the standard assay conditions previously reported (40). Both enzyme forms also catalyze a similar reaction with HEDS as substrate, with a specific activity of about 7 units/mg at pH 7.0, 5 mM HEDS, and 5 mM GSH. This disulfide appears to be one of the best substrates for the bacterial enzyme, comparable to CDNB. Notably, the C10A mutant enzyme is completely unable to utilize both $CysSO_3^-$ and HEDS as substrates indicating an essential role of this residue in the redox activity.

Steady-state Kinetics of the Thiol-disulfide Oxidoreductase Reaction—Steady-state kinetic analysis was performed with GSTB1-1ox and GSTB1-1red at pH 7.0 and 30 °C, by varying both HEDS and GSH from 0.4 to 5 mM (Fig. 4). Non-intersecting lines on the double-reciprocal plots are consistent with a ping-pong mechanism for both enzymes.

Similar kinetic behavior has been reported for a human glutaredoxin with GSS-cysteine as substrate, and in that case a simple ping-pong mechanism involving an *E*·S·SG disulfide intermediate was postulated (43).

The dependence of GSTB1-1 activity on the concentration of HEDS suggests substrate inhibition at high HEDS and low GSH concentrations. GSH concentrations higher than 1 mM removed completely the disulfide inhibition. Similar inhibition has been observed for a human glutaredoxin with all the disulfides used as substrates (44).

pH Dependence of the Thiol-disulfide Oxidoreductase Activity—Both GSTB1-1ox and GSTB1-1red exhibit an identical apparent kinetic pK_a value of 5.1 ± 0.1 (Fig. 5). As expected, the pH dependence of the spontaneous reaction, which is rate-limited by the nucleophilic displacement of the substrate by free GSH, shows a pK_a value ≥ 7.5. The pK_a value found for the enzymatic reaction is close to the pK_a of the bound GSH (see Fig. 1) thus suggesting that the nucleophilic attack of GSH thiolate to the substrate mixed disulfide may be the rate-limiting step in catalysis. A possible catalytic mechanism is reported in Scheme 3, involving a small amount of reduced enzyme in fast exchange with the disulfide substrate.

The overall proposed mechanism for GSTB1-1red is identical to GSTB1-1ox except for the first catalytic cycle, which starts from step 3 of Scheme 3.

The above mechanism agrees with the following kinetic data: (*a*) Cys-10 is an essential residue for the redox activity; (*b*) identical specific activities have been found for GSTB1-1ox and GSTB1-1red; (*c*) the enzyme in the reduced form reacts rapidly with the disulfide substrate forming a mixed disulfide with Cys-10 (35); (*d*) the rate-limiting step is the chemical event *i.e.* the nucleophilic attack of GSH thiolate to *E*·S·SR; and (*e*) steady-state kinetics is compatible with a ping-pong mechanism.

Concluding Remarks—The bacterial enzyme GSTB1-1 may be proposed as a model of a "transition enzyme" between the GST superfamily and the thiol-disulfide oxidoreductase superfamily. The co-existence in this enzyme of a conjugation activity together with a redox activity toward disulfides is not the sole indication that supports this idea; the presence of a functional cysteine residue in the active site of GSTB1-1 (absent in the recently evolved GSTs) is reminiscent of the essential cysteine found in the active site of the thioredoxin and glutaredoxin enzymes (37, 38). Other findings presented in this report and briefly commented below support this hypothesis and possibly reveal the evolutionary strategy adopted by the GST superfamily to evolve from a primitive redox enzyme into a conjugating enzyme.

GSH Binding and Activation—The bacterial enzyme has not optimized its interaction with GSH. In fact, GSTB1-1 binds GSH by a simple bimolecular interaction, whereas the more recently evolved GSTs adopt a multistep binding mechanism (23, 24) that likely represents an evolutionary advantage in terms of increased velocity toward the final Michaelis complex (25). A very premature mode of GSH binding has been found in the native GSTB1-1ox where the presence of an additional GSH molecule in the active site results in k_{on} and k_{off} values 100-fold lower than those shown by GSTB1-1red. An important

observation is that the presence of the mixed disulfide Cys-10-SG does not affect remarkably the affinity of the enzyme for free GSH, but the binding mechanism is complicated by an apparent futile redox cycle in which the external GSH rapidly exchanges with the GSH bound to Cys-10, and the enzyme remains mainly in an oxidized form (see Scheme 2). The transient co-existence of two GSH molecules in the G-site of the GSTB1-1ox·GSH complex, not evident in the crystal structure but strongly supported by the present and previous data (35), is perhaps the most peculiar property of the bacterial enzyme. This evidence is reminiscent of the first plant GST structure (45) showing two *S*-hexyl GSH molecules per active site; the GSH portion of one inhibitor binds with multiple interactions, whereas the tripeptide moiety of the second inhibitor shows only a weak interaction with the active site.

If the binding mechanism of GSTB1-1 reflects that of an ancient and primitive enzyme, it is surprising that the ability of this enzyme to activate the bound GSH is similar or even better than that seen in the more recently evolved GSTs. The stabilization of the GSH thiolate is achieved in the latter GSTs by means of a hydrogen bond interaction between the sulfur atom of GSH and the hydroxyl group of strictly conserved Tyr or Ser residues. In the case of GSTB1-1, replacement of Tyr-5 and Ser-9 residues (the bacterial counterpart of the conserved Tyr and Ser residues in the Pi, Alpha, Mu, and Theta GSTs) did not cause any shift of the pH dependence of the k_{cat}/K_m^{CDNB} (33), suggesting these residues are not involved in the GSH activation. On the other hand, the present data indicate that the sulfur atom of Cys-10 (both in the sulfhydryl and in the disulfide form) plays a clear role in the GSH activation; in fact its replacement by alanine causes an increase of the GSH pK_a value. The involvement of Cys-10 in the GSH activation is also confirmed by the x-ray crystal structure showing the sulfur atom of this residue close to the position of the hydroxyl atom of the Tyr and Ser residues in the other classes, although the peptide main-chain atoms are in different positions (19).

Catalytic Mechanism—The classic conjugation activity catalyzed by the more recently evolved GSTs is also observed in both GSTB1-1ox and GSTB1-1red, but it occurs at low efficiency. The specificity constant k_{cat}/K_m is about 10^3 M^{-1} s^{-1} for both GSTB1-1ox and GSTB1-1red, while the k_{cat}/K_m value observed in Alpha, Pi, and Mu GSTs is about 5×10^5 M^{-1} s^{-1}. In particular, the chemical step (which is rate-limiting in catalysis) appears to be not optimized in GSTB1-1. In this context, the Cys-10 residue may play a role in the correct orientation of the two substrates, the effect depending on the nature of the co-substrate. In fact, its replacement by alanine causes a 50-fold decrease of the catalytic rate, by using NBD-Cl, whereas an almost unchanged activity is recovered by using CDNB.

Unlike the conjugation activity, the additional thiol-disulfide oxidoreductase reaction performed by GSTB1-1 requires a direct involvement of Cys-10 in the catalytic mechanism, as suggested by the complete loss of activity observed in the C10A mutant enzyme. Apart from the mechanistic details of this reaction, which have been focused in this report (see Scheme 3) and which appear similar to those found in glutaredoxins, a much lower catalytic efficiency is evident for the bacterial enzyme. In fact, the k_{cat} of GSTB1-1 is at least one order of magnitude lower than k_{cat} values found in the thiol-disulfide oxidoreductase superfamily (44, 46).

It has been proposed that a new enzyme may evolve by selection of a "promiscuous" enzyme that acquired adventitiously a new catalytic role. Subsequent evolution enhances the new reaction at the expense of the old reaction (47). In this context, the promiscuous GSTB1-1 appears like a snapshot in the evolutionary pathway from a redox enzyme into a conjugating enzyme (Fig. 6). In fact, the structural similarity between the active sites of GSTB1-1 and glutaredoxins has been already underscored (19), and the redox and conjugation catalyzes are not optimized in GSTB1-1. Probably, the evolution from the thiol-disulfide oxidoreductase to the GST superfamily involved the selective modification of an ancestral active site already able to bind and activate the GSH molecule. Replacement of the cysteine residue (essential for the redox catalysis) by a tyrosine residue (like observed in the more recently evolved GSTs) might have been the crucial step in this evolutionary pathway.

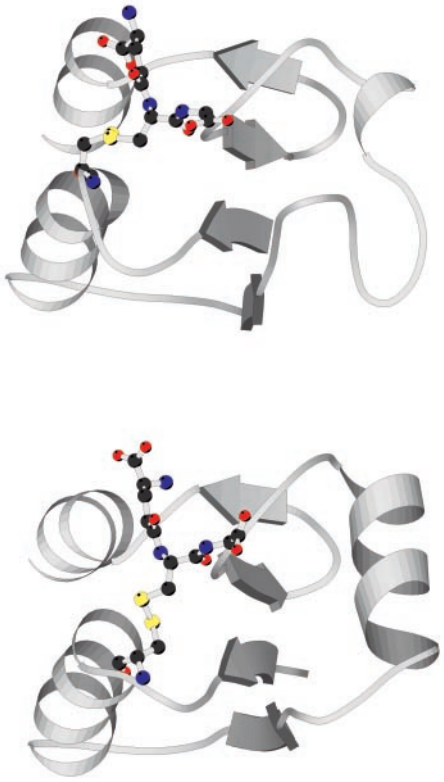

FIG. 6. **Structural relationship between GSTB1-1 and glutaredoxin.** Structure of GSTB1-1 (Protein Data Bank code 1PMT (19)). Ribbon representation of the N-terminal domain indicating the location of secondary structure. Disulfide-bound GSH to Cys-10 is *highlighted* in *ball-and-stick* fashion (*upper model*). Structure of *E. coli* glutaredoxin 3 (Protein Data Bank code 3GRX (48)). Ribbon representation, shown in approximately the same orientation as in GSTB1-1 structure, indicating the location of secondary structure. For clarity, C-terminal residues 74–82 have been omitted. Disulfide-bound GSH to Cys-11 is *highlighted* in *ball-and-stick* fashion (*lower model*). The graphics were produced using MOLSCRIPT (49).

REFERENCES

1. Jakoby, W. B., and Habig, W. H. (1980) in *Enzymatic Basis of Detoxification* (Jakoby, W. B., ed) Vol. 2, pp. 63–94, Academic Press, New York
2. Armstrong, R. N. (1997) *Chem. Res. Toxicol.* **10,** 2–18
3. Mannervik, B., Alin, P., Guthenberg, C., Jensson, H., Tahir, M. K., and Jornvall, H. (1985) *Proc. Natl. Acad. Sci. U. S. A.* **82,** 7202–7206
4. Di Ilio, C., Aceto, A., Piccolomini, R., Allocati, N., Faraone, A., Cellini, L., Ravagnan, G., and Federici, G. (1988) *Biochem. J.* **255,** 971–975
5. Toung, Y.-P. S., Hsieh, T.-S., and Tu, C.-P. D. (1993) *J. Biol. Chem.* **268,** 9737–9746
6. Meyer, D. J., Coles, B., Pemble, S. E., Gilmore, K. S., Fraser, G. M., and Ketterer, B. (1991) *Biochem. J.* **274,** 409–414
7. Buetler, T. M., and Eaton, D. I. (1992) *Environ. Carcinogen. Ecotoxicol. Rev.* **10,** 181–203
8. Meyer, D. J., and Thomas, M. (1995) *Biochem. J.* **311,** 739–742
9. Pemble, S. E., Wardle, A. F., and Taylor, J. B. (1996) *Biochem. J.* **319,** 749–754
10. Board, P. G., Baker, R. T., Chelvanayagam, G., and Jermiin, L. S. (1997) *Biochem. J.* **328,** 929–935
11. Board, P. G., Coggan, M., Chelvanayagam, G. Easteal, S., Jermiin, L. S., Schulte, G. K., Danley, D. E., Hoth, L. R., Griffor, M. C., Kamath, A. V., Rosner, M. H., Chrunyk, B. A., Perregaux, D. E., Gabel, C. A., Geoghegan, K. F., and Pandit, J. (2000) *J. Biol. Chem.* **275,** 24798–24806
12. Dirr, H. W., Reinemer, P., and Huber, R. (1994) *Eur. J. Biochem.* **220,** 645–661

13. Wilce, M. C. J., and Parker, M. W. (1994) *Biochim. Biophys. Acta* **205,** 1–18
14. Raghunathan, S., Chandross, R. J., Kretsinger, R. H., Allison, T. J., Penington C. J., and Rule, G. S. (1994) *J. Mol. Biol.* **238,** 815–832
15. Wilce, M. C. J., Board, P. G., Feil, S. C., and Parker, M. W. (1995) *EMBO J.* **14,** 2133–2143
16. Cameron, A. D., Sinning, I., L'Hermite, G., Olin, B., Board, P. G., Mannervik, B., and Jones, T. A. (1995) *Structure* **3,** 717–727
17. Rossjohn, J., McKinstry, W. J., Oakley, A. J., Verger, D., Flanagan, J., Chelvanayagam, G., Tan, K.-L., Board, P. G., and Parker M. W. (1997) *Structure* **6,** 309–322
18. Oakley, A. J., Lo Bello, M., Battistoni, A., Ricci, G., Rossjohn, J., Villar, H. O., and Parker, M. W. (1997) *J. Mol. Biol.* **274,** 84–100
19. Rossjohn, J., Polekhina, G., Feil, S., Allocati, N., Masulli, M., Di Ilio, C., and Parker, M. W. (1998) *Structure* **6,** 721–734
20. Nishida, M., Harada, S., Noguchi, S., Satow, Y., Inoue, H., and Takahashi, K. (1998) *J. Mol. Biol.* **281,** 135–147
21. Graminski, G. F., Kubo, Y., and Armstrong, R. N. (1989) Biochemistry **28,** 3562–3568
22. Liu, S., Zhang, P., Ji, X., Johnson, W. W., Gilliland, G. L., and Armstrong, R. N. (1992) *J. Biol. Chem.* **267,** 4296–4299
23. Caccuri, A. M., Lo Bello, M., Nuccetelli, M., Nicotra, M., Rossi, P., Antonini, G., Federici, G., and Ricci, G. (1998) *Biochemistry* **37,** 3028–3034
24. Caccuri, A. M., Antonini G., Board, P. G., Parker, M. W., Nicotra, M., Lo Bello, M., Federici, G., and Ricci, G. (1999) *Biochem. J.* **344,** 419–425
25. Caccuri, A. M., Antonini G., Board, P. G., Flanagan, J., Parker, M. W., Paolesse, R., Turella, P., Federici, G. Lo Bello, M., and Ricci, G. (2001) *J. Biol. Chem.* **276,** 5427–5431
26. Mannervik, B. (1986) *Chem. Scr.* **26,** 281–284
27. Litwach, G., Ketterer, B., and Arias, I. M. (1971) *Nature* **234,** 466–477
28. Piredda, L., Farrace, M. G., Lo Bello, M., Malorni, W., Melino, G., Petruzzelli, R., and Piacentini, M. (1999) *FASEB J.* **13,** 355–364
29. Adler, V., Yin, Z., Fuchs, S. Y., Benezra, M., Rosario, L., Tew, K. D., Pincus, M., R., Ardana, M., Henderson, C. J., Wolf, C. R., Davis, R. J., and Ronai, Z. (1999) *EMBO J.* **18,** 1321–1334
30. Kampranis, S. C., Damianova, R., Atallah, M., Toby, G., Kondi, G., Tsichlis, P. N., and Mahkris, A. M. (2000) *J. Biol. Chem.* **275,** 29207–29216
31. Dulhunty, A., Gage, P., Curtis, S., Chelvanayagam, G., and Board, P. (2001) *J. Biol. Chem.* **276,** 3319–3323
32. Perito, B., Allocati, N., Casalone, E., Masulli, M., Dragani, B., Polsinelli, M., Aceto, A., and Di Ilio C. (1996) *Biochem. J.* **318,** 157–162
33. Casalone E., Allocati, N., Ceccarelli, I., Masulli, M., Rossjohn, J., Parker, M. W., and Di Ilio C. (1998) *FEBS Lett.* **423,** 122–124
34. Allocati, N., Cellini, L., Aceto, A., Iezzi, T., Angelucci, S., Robuffo, I., and Di Ilio C. (1994) *FEBS Lett.* **354,** 191–194
35. Caccuri, A. M., Antonini, G., Allocati, N., Di Ilio, C., Innocenti, F., De Maria, F., Parker, M. W., Masulli, M., Polizio, F., Federici, G., and Ricci G. (2002) *Biochemistry* **41,** 4686–4693
36. Martin, J. (1995) *Structure* **3,** 245–250
37. Chivers, P. T., and Raines, R. T. (1997) *Biochemistry* **36,** 15810–15816
38. Srinivasan U., Mieyal, P. A., and Mieyal, J. J., (1997) *Biochemistry* **36,** 3199–3206
39. Gill, S. C., and von Hippel, P. H. (1989) *Anal. Biochem.* **182,** 319–326
40. Axelsson, K., Eriksson, S., and Mannervik, B. (1978) *Biochemistry* **17,** 2978–2984
41. Segel, I. H. (1975) in *Enzyme Kinetics*, pp. 460–461, John, Wiley & Sons, Inc., New York
42. Ricci, G., Caccuri, A. M., Lo Bello, M., Rosato, N., Mei, G., Nicotra, M., Chiessi, E., Mazzetti, A. P., and Federici, G. (1996) *J. Biol. Chem.* **271,** 16187–16192
43. Gravina, S. A., and Mieyal, J. J. (1993) *Biochemistry* **32,** 3368–3376
44. Mieyal, J. J., Starke, D. W., Gravina, S. A., and Hocevar, B. A. (1991) *Biochemistry* **30,** 8883–8891
45. Reinemer, P., Prade, L., Hof, P., Neuefeind, T., Huber, R., Zettl, R., Palme, K., Schell, J., Koelln, I., Bartunik, H. D., and Bieseler, B. (1996) *J. Mol. Biol.* **255,** 289–309
46. Mieyal, J. J., Starke, D. W., Gravina, S. A., Dothey, C., and Chung, J. S. (1991) *Biochemistry* **30,** 6088–6097
47. Schmidt, D. M. Z., Hubbard, B. K., and Gerlt, J. A. (2001) *Biochemistry* **40,** 15707–15715
48. Nordstrand, K., Åslund, F., Holmgren, A., Otting, G., and Berndt, K. D. (1999) *J. Mol. Biol.* **286,** 541–552
49. Kraulis, P. (1991) *J. Appl. Crystallogr.* **24,** 946–950

GSTB1-1 from *Proteus mirabilis* : A SNAPSHOT OF AN ENZYME IN THE EVOLUTIONARY PATHWAY FROM A REDOX ENZYME TO A CONJUGATING ENZYME

Anna Maria Caccuri, Giovanni Antonini, Nerino Allocati, Carmine Di Ilio, Francesca De Maria, Federica Innocenti, Michael W. Parker, Michele Masulli, Mario Lo Bello, Paola Turella, Giorgio Federici and Giorgio Ricci

J. Biol. Chem. 2002, 277:18777-18784.
doi: 10.1074/jbc.M201137200 originally published online March 11, 2002
